Embedded-atom method: Derivation and application to impurities, surfaces, and other defects in metals

Murray S. Daw and M. I. Baskes
Sandia National Laboratories, Livermore, California 94550
(Received 17 October 1983)

We develop the embedded-atom method [Phys. Rev. Lett. 50, 1285 (1983)], based on density-functional theory, as a new means of calculating ground-state properties of realistic metal systems. We derive an expression for the total energy of a metal using the embedding energy from which we obtain several ground-state properties, such as the lattice constant, elastic constants, sublimation energy, and vacancy-formation energy. We obtain the embedding energy and accompanying pair potentials semiempirically for Ni and Pd, and use these to treat several problems: surface energy and relaxation of the (100), (110), and (111) faces; properties of H in bulk metal (H migration, binding of H to vacancies, and lattice expansion in the hydride phase); binding site and adsorption energy of hydrogen on (100), (110), and (111) surfaces; and lastly, fracture of Ni and the effects of hydrogen on the fracture. We emphasize problems with hydrogen and with surfaces because none of these can be treated with pair potentials. The agreement with experiment, the applicability to practical problems, and the simplicity of the technique make it an effective tool for atomistic studies of defects in metals.

I. INTRODUCTION

The energy and structure of impurities, surfaces, and other defects in metals draw considerable attention and effort from the physics community.[1-5] The experimental investigations in these areas are often aided by complementary theoretical work. The theories are, however, frequently plagued by inherent or practical limitations. Band theories[6] are generally limited by basis-set size and the requirement of periodicity.[7,8] Cluster methods[9] are also limited by the size of clusters or basis sets permitted by computers. In both the band-theoretical and cluster approach, the total energy is given as a sum of many one-electron energies; in these methods, one solves for many eigenvalues only to produce one number in result. Alternatively, two-body interatomic potentials may be derived from fundamental considerations[10-12] or by empirical means.[13,14] These pair-potential methods, while yielding the total energy directly, require the use of an accompanying volume-dependent energy[15] to describe the elastic properties of a metal. Any ambiguity about the volume may automatically invalidate the results of a pair-potential calculation because the elastic properties of the solid are not accurately represented. Such ambiguities arise in calculations involving surfaces, for example, because the exact termination of the volume on an atomic scale at the surface is ambiguous. Relaxations, reconstructions, or defects in the surface simply make this ambiguity more pronounced. In fracture calculations, where internal surfaces are formed, one does not know whether to include the volume of the crack with the volume of the solid and, if so, to what extent. Furthermore, whereas pair potentials have been used successfully to treat inert impurities, such as He in metals,[16] the method is not applicable to chemically active impurities. It has been demonstrated[17] in particular that the energy of a hydrogen atom in a transition-metal cluster cannot be represented by pair interactions, whereas the energy of a helium atom can be so represented.

We describe here a new method, which we call the embedded atom method,[1] of treating metallic systems where fractures, surfaces, impurities, and alloying additions can be included. This new method is based on an earlier theory, the quasiatom[18] (or effective medium[19]) theory. The advent of the quasiatom method partly overcame the difficulty of treating impurities such as H in metals.[20-24] In this scheme, an impurity is assumed to experience a locally uniform, or only slightly nonuniform, environment. In its simplest form, the energy of the quasiatom is given by

$$E_{\text{quas}} = E_Z(\rho_h(R)) , \tag{1}$$

where $\rho_h(R)$ is the electron density of the host without impurity at R, the site where the impurity is to be placed, and E_Z is the quasiatom energy of an impurity with atomic number Z. Host-lattice relaxations can be treated by calculating a lattice energy from pair potentials and adding this to the quasiatom energy, so that $E_{\text{tot}} = E_{\text{quas}} + E_{\text{lat}}$,[21] but this does not circumvent the problem of defining the volume of the host. This problem precludes the treatment of many interesting problems, such as fracture and hydrogen embrittlement.

We describe here the derivation and some applications of the embedded atom method, based on the quasiatom scheme, where *all* atoms are viewed as being embedded in the host consisting of all other atoms. The embedding energy is electron-density dependent, where the density is always definable, and so the problem of defining the volume is circumvented. This makes it possible for the first time to treat chemically active as well as inert impurities and alloying additions in one unified theory that can furthermore handle crystal structures which include surfaces and

cracks. The embedded-atom method is not significantly more complicated to use than pair potentials.

We begin, in the next section, by using the embedding energy to derive the form of the total energy. Certain properties of the solid are then related to the embedding energy. In Sec. III, we show how the functions arising in the theory can be obtained by empirical means. This semiempirical method is then applied in Sec. IV to several problems involving surfaces and hydrogen. Finally, in Sec. V, we discuss the results.

II. THEORY

Each atom in a solid can be viewed as an impurity embedded in a host comprising all the other atoms. Because the energy of an impurity is a functional of the electron density of the unperturbed (i.e., without impurity) host (as will be reviewed in this section), the cohesive energy of a solid can be calculated from the embedding energy. In this section we will make some reasonable approximations to allow practical application of this view.

In principle, it is possible, of course, to obtain the electron density established by a given potential, and the energy is then a functional of that potential. Hohenberg and Kohn[25] show the converse: that the electron density uniquely specifies the potential (to within an additive constant), and thus the energy is a functional of the density. Thus the unperturbed host potential is determined by its electron density. When an impurity is introduced, the total potential is a sum of host and impurity potentials, so the energy of the host with impurity is a functional of the host and impurity potentials. Because the host potential is uniquely determined by the unperturbed host electron density, and the impurity potential is set by the position and charge of the impurity nucleus, the energy of the host with impurity is a functional of the *unperturbed* host electron density and a function of the impurity type and position (first stated by Stott and Zaremba[18]). That is,

$$E=\mathcal{F}_{Z,R}[\rho_h(r)]\ , \tag{2}$$

where $\rho_h(r)$ is the unperturbed host electron density, and Z and R are the type and position of the impurity. This corollary is to be distinguished from the Hohenberg-Kohn theorem, which shows that the total energy is a functional of the total electron density. Rather, the new statement is that the energy of an impurity is determined by the electron density of the host *before* the impurity is added.

It is important to understand that the Stott-Zaremba corollary, stated in Eq. (2), is *not* a means of solving for the self-consistent density around an impurity; that is, unlike the Hohenberg-Kohn theorem, it is *not* a variational theorem. Instead, it states that the fully self-consistent calculation of the energy will depend on the initial, unperturbed host electron density, which is the argument of the functional $\mathcal{F}$. Therefore, self-consistency is contained implicitly, not explicitly, in Eq. (2).

The functional $\mathcal{F}$ is a universal functional, independent of host. Its form is unknown, and is probably rather complicated. A simple approximation would be to assume that the energy depends only on the limited environment immediately around the impurity (Nørskov[19]), or equivalently that the impurity experiences a locally uniform electron density (the uniform-density approximation of Stott and Zaremba[18]). This simplification can be viewed either as a local approximation, or as the lowest-order term involving the successive gradients of the density. In the extreme case, Eq. (2) takes the form of Eq. (1), where F is now a function and the host density is sampled only at the impurity position.

At this level of approximation, the impurity problem is identical to that of an impurity in jellium. The position dependence is trivial in Eq. (2), so that the energy depends only on the density of the background electron gas. Puska *et al.*[26] have calculated the energies of all atoms from the first three rows of the Periodic Table in a homogeneous electron gas as functions of the background density. They find two classes of behavior. The rare-gas atoms have their lowest energies in a background of vanishing density, and the energies are linear in the density. The chemically active elements have a linear region at high densities, but have a single minimum at lower densities, the depth of which is correlated with the chemical bond strengths typical of bonds formed with that element.[26]

Note that the linearity of the energy for the full range of ρ indicates the chemical inactivity of an atom. It will be shown later that as a linear function, the energy is approximated very well by a pair interaction. It is also true that for nonlinear functions, the impurity generally cannot be treated with pair potentials. The quasiatom—uniform-density approximation thereby indicates that pair potentials are inadequate for chemically active elements,[17] whereas the quasiatom energy does reflect certain chemical effects.

Because each atom can be viewed as an impurity in the host of other atoms, we could take the following ansatz, based on the quasiatom concept, for the total energy,

$$E_{\rm tot}=\sum_i F_i(\rho_{h,i})\ , \tag{3}$$

where F_i is the *embedding energy*, $\rho_{h,i}$ is the density of the host at the position R_i but without atom i, and the total energy is the sum of the individual contributions, Here each atom is assumed to experience a locally uniform electron gas, and the embedding energy is defined to be the energy of that atom in a uniform electron gas relative to the atom separated from the electron gas.

The embedding function F is *not* trivially related to the functional $\mathcal{F}$ in Eq. (2). The above ansatz is more than a simple generalization of the quasiatom concept. In terms of the functional $\mathcal{F}$ in Eq. (2), the energy required to remove an atom from a solid, leaving a vacancy (neglecting lattice relaxations for now), is given simply by

$$E=\mathcal{F}_{\rm atom}[\rho_{\rm solid}(r)]\ , \tag{4a}$$

where the "solid" here includes the vacancy. It must also be true that the same energy must be obtained by viewing the solid with vacancy as the *impurity* and the single atom as the *host,* so that

$$E=\mathcal{F}_{\rm solid}[\rho_{\rm atom}(r)]\ . \tag{4b}$$

On the other hand, the embedding ansatz [Eq. (3)] prescribes that the energy to remove an atom from a solid

is given by

$$E=\sum_i [F_i(\rho_i^*)-F_i(\rho_i)] , \tag{4c}$$

where the sum is over all atoms except the one removed, and ρ_i^* is the density at atom i in the solid with the vacancy. These three expressions [(4a), (4b), and (4c)] for the energy must, of course, be equal. It is easily seen, then, that the relationship between the embedding function defined in Eq. (3) and the functional $\mathcal{F}$ is not trivial.

It is shown below that Eq. (3) leads to unrealistic properties of the solid. The origin of this difficulty lies with the assumption of extreme locality, or complete uniformity, and of a uniform positive background. That is, a real solid differs from jellium in that the charge densities are nonuniform. The corrections which involve the gradients of the density,[18] or equivalently, the sampling by the impurity of a finite region of the host,[19] serve to modify the function $F(\rho_{h,i})$ by changing the argument to a density averaged over a finite region. Also, when the uniform positive background is removed, the first-order correction is proportional to the density of the background,[19] and this can also be viewed as a modification of F. Also, Eq. (3) neglects the core-core repulsion. The correction for core-core repulsion is assumed here to take the form of a short-range pairwise repulsion between the cores. The resulting total energy is given by

$$E_{\rm tot}=\sum_i F_i(\rho_{h,i})+\tfrac{1}{2}\sum_{\substack{i,j\\ i\neq j}} \phi_{ij}(R_{ij}) , \tag{5}$$

where ϕ_{ij} is the short-range (doubly screened[18]) pair potential and R_{ij} is the distance between atoms i and j. If we make a further simplification by assuming that the host density ($\rho_{h,i}$) is closely approximated by a sum of the atomic densities (ρ^a) of the constituents [i.e., $\rho_{h,i}=\sum_{j\,(\neq i)}\rho_j^a(R_{ij})$], the energy is then a simple function of the positions of the atoms. (Here ρ_j^a is the contribution to the density *from* atom j, where $\rho_{h,j}$ is the total host electron density *at* atom j.)

The ground-state properties of the solid can be calculated from Eq. (5) in a straightforward way. In what follows we show the results for the calculation of the lattice constant, elastic constants, vacancy-formation energy, and sublimation energy of a perfect, homonuclear crystal. Because all atoms are equivalent, $F=F_i$, $\phi=\phi_{ij}$, and $\rho=\rho_j^a$. We can define $\bar{\rho}$ to be the density at equilibrium, so that $\bar{\rho}=\rho_{h,i}$ for every i and $\bar{\rho}=\sum_m \rho(a^m)$, where the a^m are the distances between neighbors and the sum is over neighbors. Also, we define $\bar{\phi}=\sum_m \phi(a^m)$.

The lattice constant is given by the equilibrium condition

$$A_{ij}+F'(\bar{\rho})V_{ij}=0 , \tag{6}$$

where

$$A_{ij}=\tfrac{1}{2}\sum_m \phi'_m a_i^m a_j^m/a^m , \tag{7a}$$

$$V_{ij}=\sum_m \rho'_m a_i^m a_j^m/a^m , \tag{7b}$$

and where a_i^m is the ith component of the position vector to the mth neighbor, $\phi'_m=[d\phi(r)/dr]_{r=a^m}$, and $\rho'_m=[d\rho(r)/dr]_{r=a^m}$.

The elastic constants at equilibrium are given by

$$C_{ijkl}=(B_{ijkl}+F'(\bar{\rho})W_{ijkl}+F''(\bar{\rho})V_{ij}V_{kl})/\Omega_0 , \tag{8}$$

where Ω_0 is the undeformed atomic volume, and

$$B_{ijkl}=\tfrac{1}{2}\sum_m(\phi''_m-\phi'_m/a^m)a_i^m a_j^m a_k^m a_l^m/(a^m)^2 , \tag{9a}$$

$$W_{ijkl}=\sum_m(\rho''_m-\rho'_m/a^m)a_i^m a_j^m a_k^m a_l^m/(a^m)^2 , \tag{9b}$$

where $\phi''_m=[d^2\phi(r)/dr^2]_{r=a^m}$, and $\rho''_m=[d^2\phi(r)/dr^2]_{r=a^m}$.

For cubic crystals the three independent elastic constants are, in Voigt notation, as follows:

$$C_{11}=[B_{11}+F'(\bar{\rho})W_{11}+F''(\bar{\rho})(V_{11})^2]/\Omega_0 , \tag{10a}$$

$$C_{12}=[B_{12}+F'(\bar{\rho})W_{12}+F''(\bar{\rho})(V_{11})^2]/\Omega_0 , \tag{10b}$$

$$C_{44}=[B_{12}+F'(\bar{\rho})W_{12}]/\Omega_0 . \tag{10c}$$

From Eqs. (6) and (10), we can see the interplay between the pair potential and the embedding energy. If the pair potential is removed, then Eq. (6) establishes $F'(\bar{\rho})=0$, and Eqs. (10) then give $C_{11}=C_{12}$ and $C_{44}=0$, which is obviously violated in real solids. If the embedding energy is neglected, and we rely entirely on the pair potential, then the equilibrium condition gives $A_{ij}=0$, so $C_{12}=C_{44}$ (the Cauchy relation), which in general is also not valid. It is seen from Eqs. (10) that the Cauchy discrepancy ($C_{12}-C_{44}$) is determined by the curvature of F at equilibrium.

The sublimation energy is given by

$$E_s=-[F(\bar{\rho})+\tfrac{1}{2}\bar{\phi}] . \tag{11}$$

The vacancy-formation energy is

$$E_{1V}^F=-\tfrac{1}{2}\bar{\phi}+\sum_m [F(\bar{\rho}-\rho_m)-F(\bar{\rho})]+E_{\rm relax} , \tag{12}$$

where $E_{\rm relax}$ takes account of the lattice relaxation around the vacancy.

When impurities or alloys are formed, it is necessary to know the embedding function $F(\rho)$ for each element, as well as the pair potential $\phi_{ij}(r)$ for each type of pair. Given those functions, any of the ground-state properties of the impurity or alloy can be calculated. The heat of solution is one example. Another example is the migration energy of an impurity, given as the difference between the saddle-point energy and the equilibrium energy. It is especially important to include lattice relaxations in many calculations.[21]

In the special case when $F(\rho)$ is a linear function [i.e., $F(\rho)=F(0)+\rho F'$], as is the case for helium, the entire scheme is equivalent to the use of a different pair potential, $\psi(r)=\phi(r)+2\rho(r)F'$. This is consistent with the observation of Baskes *et al.*[17] that helium, but not hydrogen, in metals can be treated with a pair potential. It is also consistent with the observation that pair potentials alone cannot represent the elastic properties of real solids. This is evident here in Eqs. (10), where the Cauchy condition ($C_{12}=C_{44}$) is satisfied if the curvature of F at equilibri-

um is zero.

It is interesting to compare the pair-potential method[15] (which uses the volume-dependent term) with the embedded-atom method. In the former case, it was noted that without the volume-dependent term, there was no Cauchy discrepancy (in conflict with experiment). It was then suggested that a volume-dependent energy be added to account for the compressibility of the electron gas.[27] The pair potential provides the attraction between atoms while the volume-dependent term serves to slightly expand the solid and gives the correct elastic constants. In contrast, however, in what follows, the embedding energy, which depends on the electron density, is dominant and provides cohesion while the short-range repulsive pair interaction keeps the solid at a slightly larger lattice constant. In this way, we have replaced the traditional volume-dependent energy with a density-dependent one, the advantage being that electron density is always definable.

III. DETERMINATION OF THE FUNCTIONS F AND ϕ

At this point one could try to calculate F and ϕ from first principles for any element, including as many corrections as possible for the nonuniformity of the host electron density. However, it is not practical at this time to calculate even the energy in a uniform host (jellium) for atoms beyond the third row of the Periodic Table (this is because the resonances introduced by the d states are too narrow[28]). On the other hand, it has been shown that, at least for light atoms, the next higher corrections do not change the qualitative form of the functions.[18,19] Assuming that the complete theory retains the qualitative form of the lower-order functions, one can establish F and ϕ empirically from the physical properties of the solid. We have done this using the lattice constant, elastic constants, vacancy-formation energy, and sublimation energy in fcc and bcc phases to determine the functions.

Because $F(\rho)$ and $\phi(r)$ for each element are determined from the properties of the corresponding pure metal, all that remains for alloy calculations is the determination of the unlike atom-pair interaction. In many types of repulsive pair potentials it is found that ϕ_{ij} is equal to the geometrical mean of ϕ_{ii} and ϕ_{jj}.[29–31] This is equivalent to assigning a particular form to ϕ_{ij}:

$$\phi_{ij}(r)=Z_i(r)Z_j(r)/r\ , \tag{13}$$

in order to represent the interactions of two neutral, screened atoms, as suggested by the origin of ϕ as an electrostatic energy. Generally, then, for each element M we seek two functions: the embedding energy $F_M(\rho)$ and the effective charge $Z_M(r)$.

We have determined the functions $F(\rho)$ and $Z(r)$ for Ni and Pd as examples. These are shown in Figs. 1 and 2. The experimental physical constants used in the fit are compared in Table I to the fitted values. The fit is sensitive only to the range of densities from zero to slightly above the equilibrium density and is well within experimental uncertainties. The functions are cubic splines, for generality, and the spline knots are tabulated in Table II.

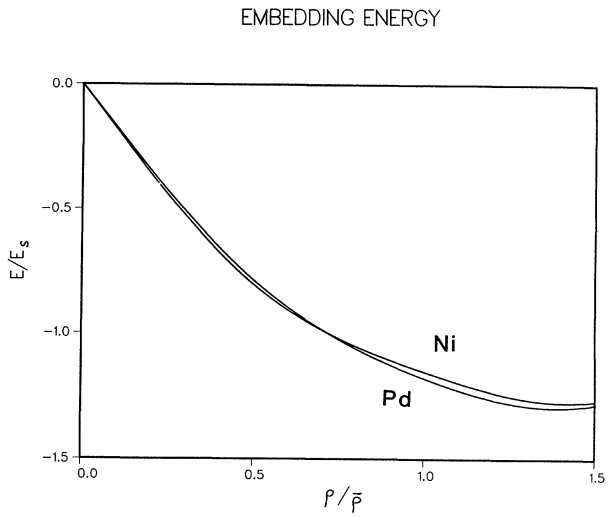

FIG. 1. Embedding energies for Ni and Pd as functions of background electron density. The functions for Ni and Pd were determined semiempirically, as explained in the text. The energies are scaled by the sublimation energy and the densities by the equilibrium density (see text).

Constraints were imposed upon F to give it the same qualitative form it had in the functions calculated by Puska *et al.*[26] (i.e., F has a single minimum and F is linear at higher densities). In addition, to make the zero of energy correspond to neutral atoms separated to infinity, the function was constrained to go to zero at vanishing density. The constraints upon $Z(r)$ required that it be monotonic and vanish continuously beyond a certain distance. The cutoff distance chosen was the shortest possible one which permitted a reasonable fit, which in this case (fcc metals) was between first and second neighbors.

The vacancy relaxation energy is calculated (in the manner described in Sec. IV) to be 0.01 eV and is rather insensitive to the fit. This simplifies the fitting to the vacancy-formation energy.

An ambiguity arises from the unknown state of the

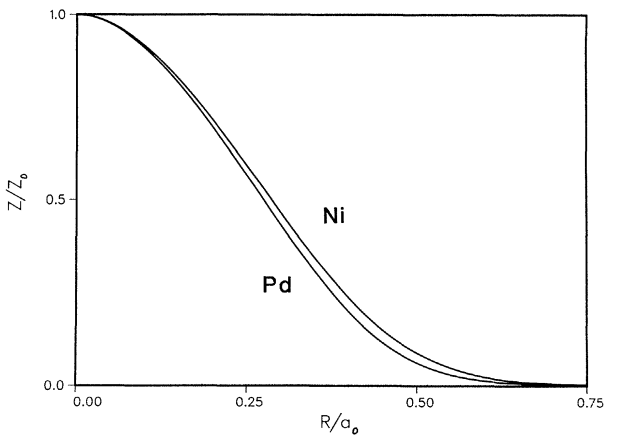

FIG. 2. Effective charges for Ni and Pd. The functions were determined semiempirically, as explained in the text. The charge is scaled by the total nuclear charge and the distance by the lattice constant.

TABLE I. Quantities used for determination of the functions $F(\rho)$ and $Z(r)$ for Ni and Pd, and their fitted values. Lattice constant a_0 in Å; elastic constants C_{11}, C_{12}, and C_{44} in 10^{12} dyn/cm^2; sublimation energy E_s in eV; vacancy-formation energy E_{1V}^F in eV; and the energy difference between bcc and fcc phases, in eV.

	Nickel		Palladium	
	Expt.	Fit	Expt.	Fit
a_0	3.52[a]	3.52	3.89[a]	3.89
C_{11}	2.465[b]	2.438	2.341[b]	2.305
C_{12}	1.473[b]	1.506	1.761[b]	1.803
C_{44}	1.247[b]	1.278	0.712[b]	0.755
E_s	4.45[c]	4.45	3.91[c]	3.91
E_{1V}^F	1.4[d]	1.4	1.4[d]	1.4
$E_{bcc}-E_{fcc}$	0.06[e]	0.07	0.06[e]	0.05

[a]Reference 48.
[b]Reference 49.
[c]Reference 50.
[d]Reference 51.
[e]Reference 52 (the experimental number is derived from a model of experimental binary phase diagrams).

atoms in the solid. The atomic densities were taken from calculations by Clementi *et al.*[32] These calculations are based on single-determinant Hartree-Fock theory, and therefore do not allow the proper mixing between given electronic configurations ($3d^8 4s^2$, $3d^9 4s$, or $3d^{10}$ for Ni, for example). In both the isolated atom and the solid, the configuration in the true ground state is not accurately known. We have allowed for this by defining an empirical parameter N_s, which corresponds to the s-like content of the atomic density. Thus the Ni atomic density is given as a sum of s and d contributions according to $\rho^a(r)=N_s\rho_s^a(r)+(N-N_s)\rho_d^a(r)$, where N is the total number of outer electrons. This parameter N_s cannot be determined by fitting to the properties of the homonuclear material, because any change in the density can be compensated for by a change in the function $F(\rho)$, which is the only place where the density affects the energy. However, the appropriate N_s for a metal can be determined by fitting to the heat of solution of, say, hydrogen in that metal, as will be discussed in the next paragraph. This gives the effective number of s-like electrons in the solid, and this number is held fixed for other types of impurities in that metal.

TABLE II. Parameters used to define the functions $F(\rho)$ and $Z(r)$ for Ni and Pd. The positions of the spline knots and the values at the knots are given. Distances are given in Å, densities in Å^{-3}, charge in a.u., and energy in eV. The lattice constants are given in Table I. The equilibrium densities $\bar{\rho}$, defined in the text, are $\bar{\rho}=0.02855$ Å^{-3} for Ni and $\bar{\rho}=0.01518$ Å^{-3} for Pd. For $\rho>2.3\bar{\rho}$, a linear extrapolation is performed based on the slope at the last knot.

r	$Z_{Ni}(r)$	$Z'_{Ni}(r)$	$Z_{Pd}(r)$	$Z'_{Pd}(r)$
0.0	28.0	0.0	46.0	0.0
$0.43a_0$	5.054		6.658	
$0.65a_0$	0.294		0.298	
$0.71a_0$	0.137		0.153	
$0.85a_0$	0.0	0.0	0.0	0.0
ρ	$F_{Ni}(\rho)$	$F''_{Ni}(\rho)$	$F_{Pd}(\rho)$	$F''_{Pd}(\rho)$
0.0	0.0	0.0	0.0	0.0
$0.5\bar{\rho}$	−3.586		−3.117	
$1.0\bar{\rho}$	−5.148		−4.697	
$2.0\bar{\rho}$	−3.407		−3.015	
$2.3\bar{\rho}$	0.0	0.0	0.0	0.0

For impurities, we need to fix the functions $F(\rho)$ and $Z(r)$ for each element. To do so, we take the embedding energies from the calculations by Puska *et al.*,[26] without adjustment. Nørskov[19] has added corrections to the F_H of Puska *et al.*[26] which might alter the results for the problems involving hydrogen, but we will use only the original functions of Puska *et al.*[26] in this work. The quantities $Z_H(r)$ and N_s^{Ni} are determined by fitting to the heat of solution and migration energy of H in Ni. The interstitial site lowest in energy for the hydrogen is found to be the octahedral—halfway between second-nearest-neighbor metal atoms—and the migration path goes along the [111] direction to a tetrahedral site, with the saddle point being about $\frac{2}{3}$ of the way from the octahedral to tetrahedral site. (These calculations allow for the relaxation of the metal lattice, which is necessary for hydrogen-migration calculations.[20,21]) This fixes $N_s^{Ni}=0.85$. The experimental data and the calculations fitted to them are shown in Table III and functions are given in Table IV. The parameters used here for calculating $\rho_s^a(r)$ and $\rho_d^a(r)$ are given in Table V. For another metal, we can find the N_s from the hydrogen heat of solution [the $Z_H(r)$ has been determined from the fit to Ni]. For Pd, this is $N_s=0.65$ (see Table III). We can then calculate, without further adjustment in parameters, the migration energy for H in Pd. This, and other examples, are illustrated in the next section.

In summary, for each element in the calculation, we need the functions $F(\rho)$ and $Z(r)$, the Clementi functions for the atomic electron density $\rho^a(r)$, and the quantity N_s. This is how we determined them for Ni and H.

(1) $F_{Ni}(\rho)$ and $Z_{Ni}(r)$ were determined empirically from the properties of Ni such as its elastic constants, etc.

TABLE III. (a) Quantities used for determination of the function $Z(r)$ for H and N_s for Ni, and their fitted values: hydrogen heat of solution [relative to the molecular bond strength of 2.4 eV atom (Ref. 6)] and migration energy in Ni. (b) Quantity used for determination of the N_s for Pd, and its fitted value, hydrogen heat of solution (relative to the molecular bond strength) in Pd.

	Expt.	Fit
(a)		
Heat of solution (eV)	0.17[a]	0.16
Migration energy (eV)	0.41[b]	0.45
(b)		
Heat of solution	−0.10[a]	−0.12

[a]Reference 53.
[b]Reference 54.

TABLE IV. Parameters used to define the functions $F(\rho)$ and $Z(r)$ for H. The function $F_H(\rho)$ comes from fitting $F_H(\rho)=b_1\rho+b_2+1/(b_3\rho+b_4)$ to the results of Puska *et al.* (Ref. 26) $Z_H(r)=(1-r/2.0)^p$, $r<2$ and $Z_H(r)=0$, $r>Z$, where the exponent is determined by fitting to the properties listed in Table III(a). Distances are given in Å, densities in Å^{-3}, charge in a.u., and energy in eV.

$b_1=$	20.445 10
$b_2=$	−2.897 859
$b_3=$	52.897 85
$b_4=$	0.412 562
$p=$	3.83

TABLE V. Parameters used to calculate the atomic density of Ni and Pd. The total density is given by $\rho^a(r)=N_s\rho_s^a(r)+(N-N_s)\rho_d^a(r)$, where $N=10$, $N_s^{Ni}=0.85$, and $N_s^{Pd}=0.65$. The spherically averaged s- and d-like densities are computed from Clementi (Ref. 32) by

$$\rho_s^a(r)=\left|\sum_i C_i R_i(r)\right|^2/4\pi\ ,$$

$$R_i(r)=\frac{(2\zeta_i)^{(n_i+1/2)}}{[(2n_i)!]^{1/2}}r^{n_i-1}e^{-\zeta_i r}\ ,$$

and similarly for $\rho_d^a(r)$. The ζ's below are given in Å^{-1}.

i	n_i	ζ_i	C_i
		Nickel	
4s			
1	1	54.888 85	−0.003 89
2	1	38.484 31	−0.029 91
3	2	27.427 03	−0.031 89
4	2	20.882 04	0.152 89
5	3	10.957 07	−0.200 48
6	3	7.319 58	−0.054 23
7	4	3.92 650	0.492 92
8	4	2.15 289	0.618 75
3d			
1	3	12.675 82	0.421 20
2	3	5.432 53	0.706 58
		Palladium	
5s			
1	1	89.219 28	−0.000 71
2	1	61.909 83	0.024 24
3	2	40.127 41	0.168 08
4	2	38.427 03	−0.242 34
5	3	26.927 41	−0.016 86
6	3	18.397 98	0.191 78
7	4	10.683 46	−0.277 59
8	4	7.241 12	−0.022 57
9	5	4.202 29	0.552 09
10	5	2.339 89	0.570 52
4d			
1	3	29.865 60	−0.087 21
2	3	16.801 95	−0.238 76
3	4	9.020 38	0.570 74
4	4	4.671 47	0.582 01

(2) $F_H(\rho)$ for hydrogen was taken from the first-principle calculations of Puska *et al.*

(3) N_s^{Ni} and $Z_H(r)$ were determined by fitting to the hydrogen heat of solution and migration energy in Ni.

We next empirically determined the quantities $F(\rho)$ and $Z(r)$ for another metal, Pd, from its elastic constants, etc., and N_s^{Pd} was fixed by fitting to the hydrogen heat of solution. Now many other properties can be investigated without adjusting the parameters both to test the validity of the approach and to give new insight into the atomistic processes of interesting phenomena.

IV. APPLICATIONS

In this section we will apply Eq. (5) and the functions determined semiempirically in Sec. III to the following problems: surface energy and relaxation in Ni and Pd, properties of H in bulk Ni and Pd (binding of H to vacancies and surfaces, lattice expansion in the hydride phase, and, for Pd only, the migration energy), and fracture of Ni and the effects of hydrogen. Problems with hydrogen and with surfaces have been emphasized, because none of these calculations can be done with pair potentials. There are no adjustable parameters in these calculations.

Most of the calculations involve minimizing the total energy with respect to the positions of the atoms; this is accomplished by the conjugate gradients technique.[33] The forces are computed analytically from Eq. (5):

$$\vec{f}_k=-\sum_{j\,(\neq k)}(F_k'\rho_j'+F_j'\rho_k'+\phi_{jk}')\vec{r}_{jk}\ , \tag{14}$$

where $\vec{f}_k$ is the force on the kth atom and $\vec{r}_{jk}$ is the unit vector between the jth and kth atoms.

A. Clean surfaces of Ni and Pd

For surface calculations, we minimized the total energy of Ni and Pd slabs with (100), (110), and (111) surfaces. The surface energies and relaxations are calculated, and the latter are compared to experiment in Table VI. The slabs were sufficiently thick (more than 20 layers) to guarantee that surface energies and geometries were independent of thickness to better than 0.1%.

The surface energy is computed by using the energy of each atom,

$$E_i=F(\rho_{h,i})+\tfrac{1}{2}\sum_{j\,(\neq i)}\phi(R_{ij})\ , \tag{15}$$

which is the contribution of the ith atom to the total energy in Eq. (5). For atoms in the bulk, $-E_i$ is the sublimation energy [Eq. (11)], but surface atoms will have higher energy. The difference $[E_i-(-E_s)]$ summed over all atoms and divided by the area gives the total surface energy. For Ni, the (100), (110), and (111) surface energies are 1550, 1740, and 1310 erg/cm^2, respectively. These numbers compare favorably with the measured crystal-vapor surface energy[34] (1725 erg/cm^2), which represents an average of several faces, including ones not considered here. For Pd, the calculated energies for the same surfaces are 1270, 1390, 1070 erg/cm^2, in the same order as for Ni. Unfortunately, we could find no measurement for

TABLE VI. Calculated and measured surface geometries for the (100), (110), and (111) surfaces of Ni and Pd. Surface geometry is indicated by the change in the spacing between first and second layers of surface atoms (in Å) from bulk-terminated value.

Surface	Δz_{12}(theory)	Δz_{12}(expt.)
Ni(100)	−0.06	0.0 ±0.02[a]
		0.0 ±0.1[b]
		+0.02 ±0.02[c]
		0.00 ±0.025[d]
		0.0 ±0.14[e]
		0.00 ±0.025[f]
Ni(110)	−0.11	−0.06 ±0.02[g]
		−0.10 ±0.02[c]
Ni(111)	−0.05	0.0 ±0.02[a]
		−0.025±0.025[c]
Pd(100)	−0.10	
Pd(110)	−0.15	
Pd(111)	−0.07	

[a]Reference 55.
[b]Reference 56.
[c]Reference 57.
[d]Reference 58.
[e]Reference 59.
[f]Reference 60.
[g]Reference 61.

comparison in Pd.

The relaxed geometries (see Table VI) agree with the available experimental data to within 0.1 Å. [The accuracy of the experimental analysis of the geometry is variously quoted as 0.01 to 0.1 Å (Ref. 35).] In particular, we note that the experiments on the (100) and (111) surfaces do not show a significant contraction relative to bulk, whereas the (110) surface shows an obvious contraction. The theoretical geometries agree with this, and are in keeping with the general trend of fcc surfaces which have small relaxations on the (100) and (111) surfaces and larger relaxations on the (110) surface.[36]

B. H in bulk Ni and Pd

We have calculated the hydrogen migration in Pd. The effective charge $Z_H(r)$ of hydrogen was determined in Sec. III by fitting to the heat of solution and migration energy in Ni, and the effective number of s-like electrons, N_s, in Pd was determined by fitting to the heat of solution in Pd. So it is interesting to calculate, without adjustment of the parameters, the migration energy in Pd, which we find to be 0.26 eV, in excellent agreement with experiments (0.26 eV).[37] The migration path is found to be the same as in Ni (see Sec. III).

The binding of H to a vacancy, relative to a bulk equilibrium (octahedral) site, is calculated to be 0.05 eV in Ni and 0.06 eV in Pd. The comparison with experiment is hampered by the difficulty of assigning observed traps to particular defects. Early experiments[38,39] tentatively identified a trap for H in Ni at 0.24 eV as belonging to a vacancy. On the basis of Nørskov's effective-medium calculations, an alternate assignment was made[40] for the vacancy as the H trap at 0.44 eV. On the other hand, hybrid quantum-cluster calculations[41] give 0.05 eV binding energy to a vacancy in Ni, although these authors claim that their calculated value is too low. In Pd, the latest work[40] has identified a 0.24-eV trap as a vacancy, mostly based on Nørskov's results. It is quite posible that the measured (0.2—0.45)-eV binding energy is to vacancy clusters rather than to actual, single vacancies. It is also likely that the binding energy to a vacancy is sensitive to the choice of $F_H(\rho)$. We have chosen the function from Puska *et al.*,[26] but Nørskov's corrected function[19] may give higher binding energy. Thus it is difficult to assess the agreement of the calculated binding energies with experiment. Another characteristic of hydrogen binding to vacancies, however, seems to be that the equilibrium position is not the center of the vacancy, but rather near a neighboring octahedral site. This has been observed experimentally[38,39] as well as theoretically.[40,41] The present calculations in Ni place the hydrogen atom 1.82 Å away from the center of the vacancy along a [100] direction (0.06 Å outward from what would be an octahedral site). In a vacancy in Pd, the calculated site is 0.13 Å outward from the octahedral site.

Another application of the model is to hydrides. The lattice constant of the fully stoichiometric hydride can easily be calculated by minimizing the total energy. In Ni the hydride lattice is calculated to be 4.5% expanded from the metal, compared with the measured 5%.[42] For PdH, the lattice expansion is calculated as 4%, where the experiment (on $PdH_{0.6}$) finds 3.5%.[42] Stoichiometry effects in the theory have not been considered here. In both metals, the agreement is quite good, especially considering that the electronic structure of metal hydrides is quite different from that of metals.[7] This agreement encourages the conclusion that the embedded-atom method provides a universal description of metal bonding.

C. H on Ni and Pd surfaces

The calculated and observed adsorption energies and binding sites for the (100), (110), and (111) surfaces are presented in Table VII and illustrated in Fig. 3. These calculations are for single-atom adsorption, whereas the best experiments for comparison are at coverages of fractions of a monolayer.

The calculated heats of adsorption on Ni surfaces are systematically about 0.25 eV too low, while on the Pd surfaces, the error is much less (0.05 eV too high on the average). The calculated adsorption sites are in complete agreement with the experimentally deduced sites (see Fig. 3 and Table VII). On the (111) surface, the Ni—H bond length has been measured by two groups as 1.57 Å (Ref.

TABLE VII. Calculated adsorption sites, bond distances, R_{M-H}, in Å, and adsorption energies relative to an isolated atom, E_a, in eV for hydrogen atoms on the (100), (110), and (111) surfaces in Ni and Pd. See Fig. 3 for illustrations of the sites.

	Theory			Experiment	
Surface	Site	R_{M-H}	E_a	Site	E_a
Ni(100)	hollow	1.73	2.66		2.90[a]
	bridge	1.59	2.54		
	top	1.54	2.26		
Ni(110)	"threefold"[b]	1.59	2.71	"threefold"[b,c]	2.87[a]
	bridge[d]	1.58	2.68		
	bridge[d]	1.66	2.63		
	top	1.53	2.34		
	hollow	1.62	2.27		
Ni(111)	hollow[e]	1.63	2.56	hollow[f,g,h]	2.87±0.03[g]
	hollow[e]	1.63	2.56		
	top	1.55	2.21		
	bridge	Unstable with respect to hollow site			
Pd(100)	hollow	1.87	2.91	hollow[i]	2.93[i]
	bridge	1.67	2.83		
	top	1.62	2.48		
Pd(110)	"threefold"[b]	1.68	3.04		2.93[j]
	bridge[d]	1.66	2.96		
	bridge[d]	1.77	2.89		
	top	1.61	2.56		
	hollow	1.70	2.37		
Pd(111)	hollow[e]	1.71	2.91	hollow[j]	2.85[j]
	hollow[e]	1.71	2.91		
	top	1.63	2.41		
	bridge	Unstable with respect to hollow site			

[a]Reference 62.
[b]The "threefold" site on the (110) surfaces does not have perfect threefold symmetry. Two of the three neighboring metal atoms are in the first layer and one is in the second, thus reducing the symmetry. But the geometry is close to what would be recognized as a threefold site.
[c]Reference 63.
[d]The first bridge site listed for the (110) surface is the twofold site between nearest neighbors (along a [110] direction). The second is the twofold site between second-nearest neighbors (along a [100] direction).
[e]There are two inequivalent, threefold-symmetric, hollow sites on the (111) surface which differ by the position of the second-layer metal atoms. However, these calculations of hydrogen adsorption show no distinguishable difference between these two sites.
[f]Reference 64.
[g]Reference 65.
[h]Reference 66.
[i]Reference 67.
[j]Reference 68.

43) and 1.84 (Ref. 44), which bracket the theoretical bond distance. Cluster calculations by Melius *et al.*[45–47] indicate Ni—H bond lengths from 1.6 to 1.8 Å, depending on surface and cluster size, in good agreement with the present work.

D. Fracture in Ni

We studied the fracture of Ni (see the first description of this in Ref. 1) by minimizing the total energy of a slab, illustrated in Fig. 4(a), which is infinite and periodic in two directions, having free (111) surfaces. A line of vacancies is created to simulate a small crack, and external forces are applied along the [111] direction to the atoms on the outer surfaces. The slip planes are (111), so in the present case, the applied stress is perpendicular to the slip directions in that plane. In this way, the fracture is constrained to be brittle. For large stresses, the crystal breaks, and the fracture stress can be established by vary-

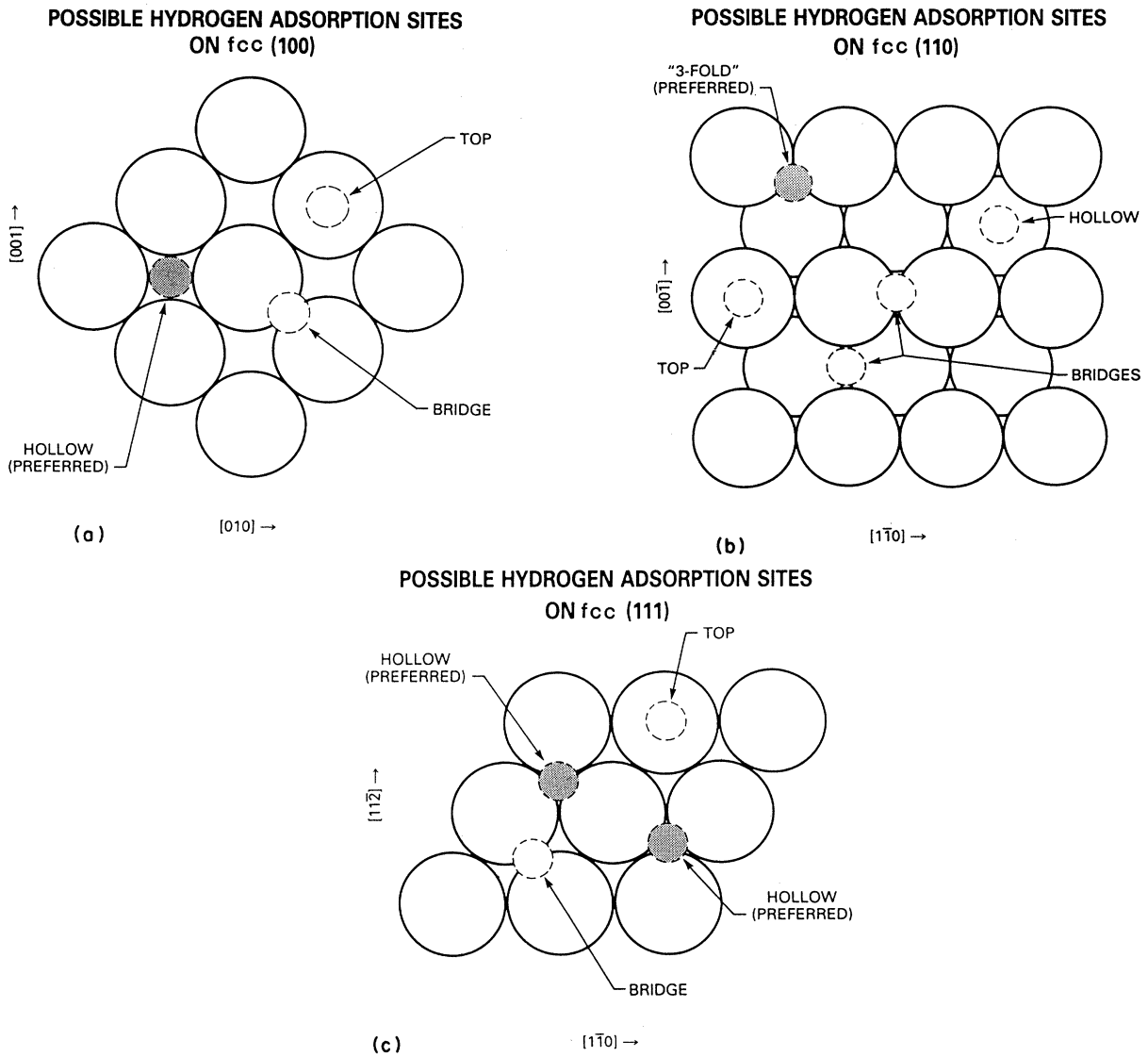

FIG. 3. Top views of the possible sites considered for hydrogen adsorption on the (100), (110), and (111) faces of an fcc crystal. The large circles represent metal atoms, the dashed circles represent hydrogen atoms in various possible sites, and the shaded hydrogen atoms represent the lowest energy sites (both experimentally and theoretically). See text and Table VII.

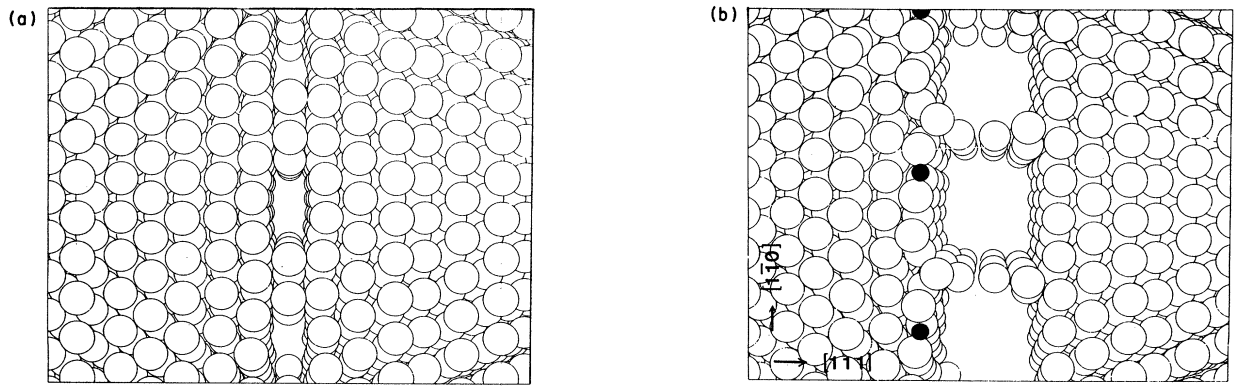

FIG. 4. Cross-sectional views of a Ni slab with defects, showing the effects of hydrogen and stress. Crystallographic directions are indicated. Open circles represent Ni atoms. Three unit cells in the vertical direction are shown, and three in the direction perpendicular to the page. (a) Four Ni atoms in each cell have been removed from the midplane and an external stress of 0.11 eV/Å^3 applied to the outer surfaces. No fracture occurs. (b) Same slab with the addition of one H atom (solid circles) per unit cell. The energy in (b) is not converged, and further iterations show the halves to be completely separated.

ing the applied stress. The crystal orientation, shown in Fig. 4(a), demonstrates brittle fracture. The introduction of H then lowers the fracture stress, and this is pictured in Fig. 4(b). It is important to emphasize that these are static calculations; dynamical effects and plasticity undoubtedly play an important role in real fracture, and these effects are under investigation.

V. CONCLUSIONS

The embedded-atom method gives a reasonable description of metallic cohesion and ground-state impurity energies. It is found that a simple embedding energy $F(\rho)$, and a short-ranged (first neighbors only) pair potential are sufficient to fit the main properties of the bulk crystal. The functions for Ni and Pd were determined by fitting to bulk properties. The resulting functions were then used to calculate energies and geometries of defects in metals, which were in good agreement with experiment. The computed surface relaxations, hydrogen-adsorption sites, and hydride lattice expansions were within 0.1 Å of experimentally determined values. The binding energy of hydrogen to vacancies and surfaces agree with experiment to within 0.25 eV. In particular, the correct hydrogen-adsorption sites on surfaces and the correct migration energy in the bulk were predicted.

The functions F and ϕ are not uniquely determined by the empirical procedure of Sec. III. In fcc metals, for example, one is able to represent the bulk properties by restricting the range of ϕ to first neighbors only, whereas such as short-ranged potential may not be the best choice in general. Until other materials can be tried (bcc metals might represent a next step), there is no way to judge the best universal forms for the embedding energy and effective charge. The choice of the best embedding function for hydrogen (Puska *et al.*[26] and Nørskov[19] are two possibilities) must also be decided on by further investigation. In the meantime, however, the model represents a very reliable way of exploring the properties of metals and impurities.

In summary, the embedded-atom method overcomes the fundamental limitations of past methods, such as pair potentials, and yet is practical enough for calculations of defects, surfaces, and impurities in metals.

ACKNOWLEDGMENT

This work was supported by the U.S. Department of Energy (Office of Basic Energy Sciences).

[1]M. S. Daw and M. I. Baskes, Phys. Rev. Lett. 50, 1285 (1983).
[2]See, for example, *Proceedings of the NATO International Symposium on the Electron Structure and Properties of Hydrodgen in Metals,* Vol. 6 of *NATO Conference Series: Materials Science,* edited by P. Jena and C. B. Satterthwaite (Plenum, New York, 1983).
[3]See, for example, W. D. Wilson, M. I. Baskes, and M. S. Daw in *Advances in the Mechanics and Physics of Surfaces,* edited by R. M. Latanision (Harwood Academic, New York, 1983).
[4]See, for example, Proceedings of the Fifth European Conference on Surface Science, edited by J. Vennik *et al.* [Surf. Sci. 126, (1983)].
[5]See, for example, *Yamada Conference V on Point Defects and Defect Interactions in Metals,* edited by J. Takamura, M. Doyama, and M. Kiritani (North-Holland, New York, 1982).
[6]J. C. Slater, *Quantum Theory of Matter,* 2nd ed. (McGraw-Hill, New York, 1968).
[7]A. C. Switendick, Solid State Commun. 8, 1463 (1970).
[8]C. D. Gelatt, H. Ehrenreich, and J. A. Weiss, Phys. Rev. B 17, 1940 (1978).
[9]R. P. Messmer, D. R. Salahub, K. H. Johnson, and C. Y. Yang, Chem. Phys. Lett. 51, 84 (1977).
[10]W. A. Harrison, *Pseudopotentials in the Theory of Metals* (Benjamin, New York, 1966).
[11]M. Rasolt and R. Taylor, Phys. Rev. B 11, 2717 (1975).
[12]M. Manninen, P. Jena, R. M. Nieminen, and J. K. Lee, Phys. Rev. B 24, 7057 (1981).
[13]M. I. Baskes and C. F. Melius, Phys. Rev. B 20, 3197 (1979).
[14]R. A. Johnson and W. D. Wilson, in *Interatomic Potentials and Simulation of Lattice Defects,* edited by P. C. Gehlen, J. R. Beeler, and R. I. Jaffee (Plenum, New York, 1971).
[15]R. A. Johnson, Phys. Rev. B 6, 2094 (1972).
[16]W. D. Wilson, Phys. Rev. B 24, 5616 (1981).
[17]M. I. Baskes, C. F. Melius, and W. D. Wilson, in *Interatomic Potentials and Crystalline Defects,* edited by J. K. Lee (Metallurgical Society of AIME, New York, 1981) (see Fig. 4 and discussion thereof).
[18]M. J. Stott and E. Zaremba, Phys. Rev. B 22, 1564 (1980).
[19]J. K. Nørskov, Phys. Rev. B 26, 2875 (1982).
[20]M. S. Daw, C. L. Bisson, and W. D. Wilson, Metall. Trans. 14a, 1257 (1983).
[21]M. S. Daw, C. L. Bisson, and W. D. Wilson, Solid State Commun. 46, 735 (1983).
[22]J. K. Nørskov, A. Houmoller, P. K. Johansson, and B. I. Lundqvist, Phys. Rev. Lett. 46, 257 (1981).
[23]J. K. Nørskov and N. D. Lang, Phys. Rev. B 21, 2131 (1980).
[24]J. K. Nørskov, Phys. Rev. Lett. 48, 1620 (1982).
[25]P. Hohenberg and W. Kohn, Phys. Rev. B 136, 864 (1964).
[26]M. J. Puska, R. M. Nieminen, and M. Manninen, Phys. Rev. B 24, 3037 (1981).
[27]K. Fuchs, Proc. R. Soc. London, Ser. A 153, 622 (1936); 157, 444 (1936).
[28]M. J. Stott (private communication).
[29]D. E. Rimmer and A. H. Cottrell, Philos. Mag. 2, 1345 (1957).
[30]A. A. Abrahamson, Phys. Rev. 133, A990 (1964).
[31]A. A. Abrahamson, Phys. Rev. 178, 76 (1969).
[32]E. Clementi and C. Roetti, *Atomic Data and Nuclear Data Tables* (Academic, New York, 1974), Vol. 14. Nos. 3 and 4.
[33]J. E. Sinclair and R. Fletcher, J. Phys. C 7, 864 (1972).
[34]M. C. Inman and H. R. Tipler, Metall. Rev. 8, 105 (1963).
[35]M. A. Chesters and G. A. Somorjai, in *Annual Review of Materials Science,* edited by R. A. Huggins, R. H. Bube, and R. W. Roberts (Annual Reviews, Palo Alto, 1975), Vol. 5.
[36]F. Jona, J. Phys. C 11, 4271 (1978).
[37]J. Völkl and G. Alefeld, in *Diffusion in Solids: Recent Developments,* edited by A. S. Nowick and J. J. Burton (Academic, New York, 1975).

[38]F. Besenbacher, J. Bøttiger, and S. M. Myers, J. Appl. Phys. 53, 3536 (1982).
[39]F. Besenbacher, J. Bøttiger, and S. M. Myers, J. Appl. Phys. 53, 3547 (1982).
[40]J. K. Nørskov, F. Besenbacher, J. Bøttiger, B. B. Nielsen, and A. A. Pisarev, Phys. Rev. Lett. 49, 1420 (1982).
[41]M. I. Baskes, C. F. Melius, and W. D. Wilson, in *Proceedings of the Third International Conference on Effects of Hydrogen on Behavior of Materials, Moran, Wyoming, 1980,* edited by I. M. Bernstein and A. W. Thompson (Metallurgical Society of AIME, New York, 1980).
[42]W. Mueller, J. P. Blackledge, and G. G. Libowitz, *Metal Hydrides* (Academic, New York, 1968).
[43]W. Ho, J. DiNardo, and E. W. Plummer, J. Vac. Sci. Technol. 17, 134 (1980).
[44]S. G. Louie, Phys. Rev. Lett 42, 476 (1979).
[45]C. F. Melius, J. O. Noell, and R. H. Stulen, J. Vac. Sci. Technol. 20, 559 (1982).
[46]C. F. Melius, R. H. Stulen, and J. O. Noell, Phys. Rev. Lett. 48, 1429 (1982).
[47]C. F. Melius (private communication).
[48]C. S. Barrett and T. B. Massalski, *Structure of Metals* (McGraw-Hill, New York, 1966).
[49]G. Simmons and H. Wang, *Single Crystal Elastic Constants and Calculated Aggregate Properties: A Handbook* (MIT Press, Cambridge, Massachusetts, 1971).
[50]*Metal Reference Book,* 5th ed., edited by C. J. Smith (Butterworths, London, 1976), p. 186.
[51]*Vacancies and Interstitials in Metals,* edited by A. Seeger, D. Schumacher, W. Schilling, and J. Diehl (North-Holland, Amsterdam, 1970).
[52]L. Kaufman and H. Bernstein, *Computer Calculation of Phase Diagrams* (Academic, New York, 1970), p. 185.
[53]P. T. Gallagher and W. A. Oates, Metall. Trans. 245, 179 (1969).
[54]J. K. Tien, in *Proceedings of the Third International Conference on Effects of Hydrogen on Behavior of Materials,* edited by I. M. Bernstein and A. W. Thompson (Metallurgical Society of the AIME, New York, 1976).
[55]K. Christmann, G. Ertl, and O. Schober, Surf. Sci. 40, 61 (1973).
[56]G. E. Laramore, Phys. Rev. B 8, 514 (1973).
[57]J. E. Demuth, P. M. Marcus, and D. W. Jepsen, Phys. Rev. B 11, 1460 (1975).
[58]P. M. Marcus, J. E. Demuth, and D. W. Jepsen, Surf. Sci. 53, 501 (1975).
[59]W. N. Unertl and M. B. Webb, Surf. Sci. 59, 373 (1976).
[60]G. Hanke, E. Lang, K. Heinz, and K. Muller, Surf. Sci. 91, 551 (1980).
[61]J. R. van der Veen, R. M. Tromp, R. G. Smeenk, and F. W. Saris, Surf. Sci. 82, 468 (1979).
[62]K. Christmann, O. Schober, G. Ertl, and M. Neumann, J. Chem. Phys. 60, 4528 (1974).
[63]T. Engel and K. H. Rieder, Surf. Sci. 109, 140 (1981).
[64]M. A. Van Hove, G. Ertl, K. Christmann, R. J. Behm, and W. H. Weinberg, Solid State Commun. 28, 373 (1978).
[65]K. Christmann, R. J. Behm, G. Ertl, M. A. Van Hove, and W. H. Weinberg, J. Chem. Phys. 70, 4168 (1979).
[66]G. Casalone, M. G. Cattania, M. Simonetta, and M. Tescari, Chem. Phys. Lett. 61, 36 (1979).
[67]R. J. Behm, K. Christmann, and G. Ertl, Surf. Sci. 99, 320 (1980).
[68]H. Conrad, G. Ertl, and E. E. Latta, Surf. Sci. 4, 435 (1974).